ABDOMINAL RADIOLOGY

MRI T2-weighted sequences-based texture analysis (TA) as a predictor of response to neoadjuvant chemo-radiotherapy (nCRT) in patients with locally advanced rectal cancer (LARC)

Filippo Crimì[1] · Giulia Capelli[2] · Gaya Spolverato[2] · Quoc Riccardo Bao[2] · Anna Florio[1] · Sebastiano Milite Rossi[1] · Diego Cecchin[3] · Laura Albertoni[4] · Cristina Campi[5] · Salvatore Pucciarelli[2] · Roberto Stramare[1]

Abstract

Purpose To determine whether MRI T2-weighted sequences-based texture analysis (TA) can predict histopathological tumor regression grade (TRG) in patients with locally advanced rectal cancer (LARC) undergoing neoadjuvant chemo-radiotherapy (nCRT).

Methods Data on patients undergoing curative-intent surgery for LARC were collected. Patients with a complete pathological response, or TRG1 according to Mandard's system were classified as responders, while patients with $TRG \geq 2$ were classified as non-responders. Tumor TA was performed on each patient's paraxial T2w MRI in both pre- and post-nCRT scans, in order to extract histograms, gray-level co-occurrence matrix (GLCM) and run-length matrix (RLM) texture parameters. For features that showed a significant difference between the two groups, a receiver operating characteristic (ROC) curve was drawn.

Results Overall, 62 patients with LARC, treated with nCRT and resective surgery at our institution between 2013 and 2019 were identified. Only post-nCRT GLCM maximum probability showed a significant difference between the two groups (2909 ± 4479 in responders vs. 6515 ± 8990 in non-responders; $p = 0.039$); at the ROC curve, Youden index showed a sensitivity of 14% and a specificity of 100% for this parameter.

Conclusions MRI T2-weighted sequences-based TA was not effective in predicting pathological complete response to nCRT in patients with LARC. Further studies are needed to thoroughly investigate the potential of MRI TA in this setting.

✉ Gaya Spolverato
gaya.spolverato@unipd.it

Filippo Crimì
filippo.crimi@uniroma1.it

Giulia Capelli
giulia.capelli1990@gmail.com

Quoc Riccardo Bao
bqr@hotmail.it

Anna Florio
a.florio72@gmail.com

Sebastiano Milite Rossi
sebamilite@gmail.com

Diego Cecchin
diego.cecchin@unipd.it

Laura Albertoni
laura.albertoni@aopd.veneto.it

Cristina Campi
cristina.campi@unipd.it

Salvatore Pucciarelli
puc@unipd.it

Roberto Stramare
roberto.stramare@unipd.it

[1] Department of Medicine-DIMED, Institute of Radiology, University Hospital of Padova, Padua, Italy

[2] Clinica Chirurgica I, Department of Surgical, Oncological and Gastroenterological Sciences (DiSCOG), University Hospital of Padova, Via Nicolò Giustiniani 2, 35128 Padua, Italy

[3] Nuclear Medicine Unit, Department of Medicine-DIMED, University Hospital of Padova, Padua, Italy

[4] Surgical Pathology and Cytopathology Unit, Department of Medicine-DIMED, University Hospital of Padova, Padua, Italy

[5] Department of Mathematics "Tullio Levi-Civita", University of Padova, Padua, Italy

Introduction

Rectal cancer represents a major cause of morbidity and mortality worldwide, accounting for about 44,000 new cases and 51,000 deaths per year in the USA [1]. Most cases are locally advanced, i.e., clinically staged T3–4 or node positive, at the time of diagnosis.

The gold standard for the treatment of locally advanced rectal cancer (LARC), according to the current guidelines, is neoadjuvant chemo-radiotherapy (nCRT) followed by total mesorectal excision (TME). Neoadjuvant therapy has shown to decrease the rate of local recurrences [2], and can lead to complete pathological response (pCR) in some cases [3, 4]. In patients achieving a clinical complete response (cCR) a rectal-sparing approach could be attempted in order to spare surgery, that in case of complete response would represent an overtreatment burdened by the risk of major complications and severe impairment on bowel function and quality of life [3, 5]. Given these premises, it is crucial to identify reliable predictors of tumor response in order to offer a patient-tailored treatment. Several clinical and molecular biomarkers have been investigated as possible predictors of response to treatment [6–9]. As for imaging, MRI may represent a valuable tool to predict response to nCRT. This technique offers relevant advantages, due to its high resolution in soft tissue analysis and the possibility of a multiparametric approach [10, 11]. MRI T2-weighted imaging, in particular, is used to assess the degree of tumor regression on the basis of morphological changes. To do so, a classification similar to Mandard's tumor regression grade (TRG) system [12], mrTRG, has been proposed, based on the hypointensity in the T2-weighted sequences of the fibrotic tissue in the lesion [13–15]. This classification showed to predict recurrence-free survival (RFS) disease-free (DFS) and overall survival (OS) [16], while in other studies, mrTRG showed a low correlation with pathological TRG [17]. In particular, the inter-observer agreement for this type of evaluation was not satisfying in TRG1 and 2 cases, which are the most relevant in the evaluation of a complete response [17], thus an automated quantitative approach for the evaluation of the T2-weighted signal intensity inside the lesion has been proposed showing a good inter-observer agreement and an excellent correspondence to the histopathological findings [18]. Taylor et al. [19] reported that more than 70% of tumor volume changes detected by T2-weighted images define tumor responses as determined by morphological evaluation by MRI.

However, these findings may underestimate the difficulty to determine the margin between residual tumor and surrounding normal tissues and to differentiate between residual tumor and fibrosis after nCRT, on the basis of morphological changes only. More sensitive and reliable MRI markers are needed to evaluate the efficacy or predict early responses to treatment in clinical practice. Some studies applied texture analysis (TA) in order to predict pCR; different T2-weighted images, DWI and PET/TC features showed a significant correlation with pathological findings [20–25] and some T2-weighted images features were found to associate with DFS, RFS, OS [22].

The aim of the present study was to evaluate the correlation of first- and second-order TA features of the primary lesion's volume in pre- and post-nCRT T2-weighted MRI images and histopathological TRG.

Methods

Patient selection

We retrospectively included consecutive patients with confirmed diagnosis of LARC who underwent nCRT followed by curative surgery at our center between 2013 and 2019. Patients with stage II and II rectal cancer, located at less than 11 cm from the anal verge, who received preoperative radiotherapy with a total dose of 50.4 Gy (in daily fractions of 1.8 Gy five times a week), with concomitant administration of 5-fluorouracil-based chemotherapy by continuous venous infusion or oral capecitabine, and who underwent pelvic MRI with a slice thickness of 3.5 mm both before and after nCRT, were included in the study. Inclusion criteria also involved the availability of the results of histopathological examination, complete with Mandard's TRG classification on the surgical specimens.

Patients who did not meet these criteria, along with all patients with poor image quality and movement artifacts, were excluded. All the patients included gave written informed consent to use imaging data for research aims.

Image acquisition

Staging and restaging of all patients were performed using a 1.5T MRI (Avanto; Siemens, Erlangen, Germany) with phased-array coils. The examination protocol included T2-weighted sagittal, oblique coronal (i.e., parallel to the long axis of the primary tumor) and oblique axial (i.e., perpendicular to the long axis of the primary tumor) images, with a repetition time (TR) of 3790–5354 ms, an echo time (TE) of 95 ms, a slice thickness of 3.5 mm, a field of view (FoV) of 320×286 mm and an image matrix of 320×257.

Histopathological examination

Histopathological examination was performed by expert pathologists, specialized in gastrointestinal diseases. For

each patient, a biopsy of the primary lesion before nCRT confirming the diagnosis of malignancy was available. Histopathologic examination on the surgical specimen included pathological tumor stage, nodal stage (in case of TME) and TRG according to Mandard's classification, with TRG1 indicating complete response and TRG5 indicating the absence of regressive changes in the tumor [12]. Patients with complete response (TRG1), were classified as "group 0," while patients with residual tumor (TRG2–5) were classified as "group 1."

Image analysis

A volume of interest (VOI) was outlined around the rectal lesion in all paraxial T2-weighted MRI slices in which the cancer appeared, in both pre- and post-nCRT examinations. VOIs were obtained for all patients by two radiologists, who manually contoured the tumor area, using a dedicated software (PMOD, PMOD Group, Zurich, Switzerland). Radiologists were not aware of the final histopathological results but had access to pre-nCRT images when evaluating post-nCRT scans. Particular attention was paid to avoid endoluminal mucus and healthy rectal wall and, in post-nCRT MRI, to recognize parietal edema caused by the effects of nCRT (see Fig. 1). Texture analysis was performed using PMOD analysis algorithms; thirty-three parameters, derived from voxel histograms, gray-level co-occurrence matrix (GLCM) and run-length matrix (RLM) analysis, were extracted for each MRI scan.

Statistical analysis

Continuous variables obtained through TA were expressed as mean ± standard deviation (SD). All parameters derived from TA of both pre- and post-nCRT scans were dichotomized based on the results of histopathological examinations. The comparison between the two groups (responders, or "group 0" vs. non- responders, or "group 1") was carried out using the Student's t test, with significance taken at $p \leq 0.05$. For parameters with a statistically significant difference between the two groups, a receiver operating characteristic (ROC) curve was drawn and Youden index was calculated. Statistical analysis was performed using the R software [26].

Results

Patient clinicopathological characteristics

Sixty-two patients, 42 males (67.7%) and 20 females (32.3%), were included in this study. Patients clinicopathological characteristics are shown in Table 1. The majority
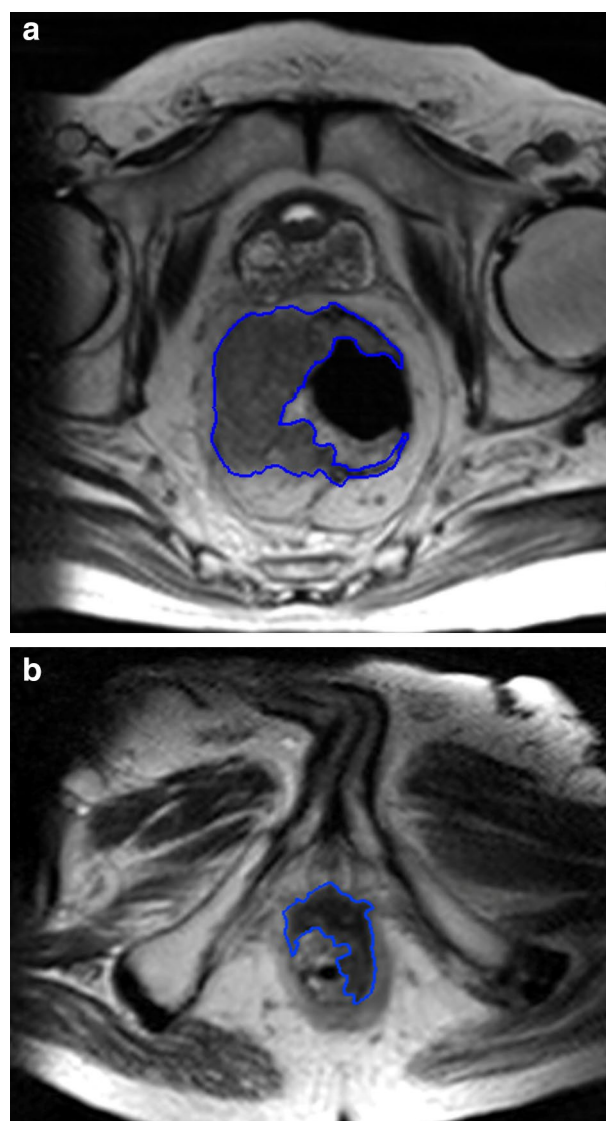

Fig. 1 a VOI manually drawn along the boundaries of a T3 rectal cancer in T2w image of staging MRI, excluding intraluminal mucus and normal rectal wall; **b** another VOI delineated around the tumor mass in a slice of a restaging MRI T2w, including both the lesion and fibrous tissue, excluding the inflammatory reaction in the nearby healthy mucosa

of patients were older than 60 years ($n = 42$, 67.7%). Fifty patients ($n = 50$, 80.6%) underwent TME, while 12 patients ($n = 12$, 19.4%) underwent transanal local excision (LE). At histopathological examination, one third of patients achieved a pCR on the primary lesion ($n = 20$, 32.3%); 24 (38.7%) were T1–T2 and the remaining were T3–T4 ($n = 18$, 29.0%). Twelve patients (19.3%) had positive lymph nodes. Overall, 19 patients were defined as responses based on pTRG = 1 (30.6%), while 43 patients with pTRG between 2 and 5 (69.4%) were defined as non-responders.

Table 1 Patient clinicopathological characteristics

Features	Classification	N (%)
Sex	Male	42 (67.7%)
	Female	20 (32.3%)
Age	≤ 60 years	20 (32.3%)
	> 60 years	42 (67.7%)
Surgery	TME	50 (80.6%)
	Local excision	12 (19.4%)
ypT	T0	20 (32.3%)
	T1	7 (11.3%)
	T2	17 (27.4%)
	T3	14 (22.6%)
	T4	4 (6.4%)
ypN	N0	38 (61.3%)
	N1	11 (17.7%)
	N2	1 (1.6%)
	Nx	12 (19.4%)
pTRG	TRG1	19 (30.7%)
	TRG2	15 (24.2%)
	TRG3	16 (25.8%)
	TRG4	9 (14.5%)
	TRG5	3 (4.8%)

ypT, histopathological T-stage after nCRT; ypN, histopathological N-stage after nCRT; pTRG, histopathological tumor regression grade according to Mandard's classification; TME, total mesorectal excision; LE, local excision. Histopathological examination of lymph nodes was not possible for patients who underwent LE; therefore, ypNx (N indeterminable) was reported for these cases

Comparison of pre-nCRT T2-weighted TA parameters

Pre-nCRT TA parameters of the two groups are reported in Table 2. None of the parameters derived from the histogram, GLCM and RLM analyses showed a statistically significant difference between the two groups. The mean pre-nCRT skewness (1.04 ± 0.51 vs. 0.79 ± 0.31) and pre-nCRT excess kurtosis (2.28 ± 1.62 vs. 1.51 ± 0.91) were lower in group 1 compared to group 0; still, the difference did not meet statistical significance ($p = 0.055$ and 0.063 respectively).

Comparison of post-nCRT T2-weighted TA parameters

Post-nCRT TA parameters for the two groups are reported in Table 3. Only GLCM maximum probability showed a statistically significant difference between the two groups (2909 ± 4479 vs. 6515 ± 8990; $p = 0.039$). Other parameters, such as GLCM homogeneity inverse different moment, GLCL sum entropy and GLCM entropy, approached the cut-off of $p = 0.05$, without reaching significance. GLCM maximum probability corresponds to occurrences of the most predominant pair of neighboring intensity values [27].

For this parameter, a ROC curve with an area under the curve (AUC) of 0.6622 (CI 95% 0.5128–0.8116) according to DeLong test was obtained [28]. The sensitivity and specificity at the Youden index were 14% and 100%, respectively (Fig. 2).

Discussion

Management of LARC is constantly evolving. During the last decades, many efforts have been made in order to reach a tailored approach in the management of this disease, thus avoiding over-treatment and preserving patient's quality of life. Non-operative management (NOM) of patients showing a cCR to nCRT can spare these patients the potential complications of major surgery, while other rectal preserving approaches, such as LE, can be used in some patients with a complete or major response in order to avoid the severe impact on quality of life of conventional surgery. On the other hand, neoadjuvant therapy itself is associated with several side effects, and is not always beneficial for the patients in terms of reduction of tumor burden.

Thus, the identification of reliable markers of response to nCRT has gained growing interest. TA has been suggested as a promising technique to investigate intra-tumor heterogeneity attributed to various factors such as hypoxia, necrosis and angiogenesis, potentially related to tumor aggressiveness and patient prognosis [20–25]. Both hypoxia and necrosis following chemo-radiotherapy cause fibrosis of the neoplastic tissue; fibrous tissue is characterized by hypo-intense signal in the T2-weighted sequences, and therefore can be differentiated from residual vital tumor [29]. TA could also predict which patients will respond to nCRT even before the treatment is started, or a few weeks after the onset of treatment [20, 21, 24, 25], and may improve MRI performance in the evaluation of response [22].

Different studies have investigated TA parameters of T2-wieghted MRI images as a tool to discriminate patients with a pCR and patients with residual disease. De Cecco et al. [20] found that only kurtosis obtained from T2-weighted pre-nCRT and mid-treatment MRI images showed significant differences between complete responders and partial or non-responders; the sensitivity and specificity for pCR prediction of the pre-nCRT T2-weighted kurtosis were 100% and 77.8%, respectively. In a later study of the same group, pretreatment T2-weighted images kurtosis showed a sensitivity and specificity with two different suggested cut-offs of, respectively, 100% and 67% and 83% and 83% [21]. Giannini et al. [23] investigated TA data in pre-nCRT MRI and 18F-FDG PET/CT images; only one second-order T2-weighted MRI texture parameter and five second-order PET texture parameters were included in a logistic regression model to differentiate responders

Table 2 Comparison of pre-nCRT T2-weighted TA parameters using Student's *t* test

Pre-nCRT parameters	Complete responders (mean)	Non-responders (mean)	*p* value
Histograms-First level TA parameters			
Mean	235.80 ± 129.67	184.99 ± 125.87	0.16
Variance	9969.51 ± 9635.84	6112.11 ± 8378.81	0.14
Skewness	1.04 ± 0.51	0.79 ± 0.31	0.06
Excess kurtosis	2.28 ± 1.62	1.51 ± 0.91	0.06
Energy	0.03 ± 0.04	0.02 ± 0.04	0.28
Entropy	3.72 ± 0.53	3.74 ± 0.53	0.87
GLCM-Second level TA parameters			
Energy angular second moment uniformity	$586,021,701 \pm 1,309,446,703$	$1,270,794,707 \pm 2,564,356,236$	0.17
Contrast inertia variance	3168.97 ± 5574.98	3216.98 ± 4539.98	0.97
Sum of squares variance	$17,731,294,744 \pm 59,403,170,934$	$46,789,306,917 \pm 183,555,401,716$	0.35
Homogeneity inverse different moment	$17,351 \pm 23,096$	$27,714 \pm 31,604$	0.15
Sum average	$57,373.94 \pm 85,882.22$	$76,980.92 \pm 78,444.54$	0.4
Sum variance	$8,845,085 \times 108 \pm 34,232,832 \times 108$	$11,825,102 \times 108 \pm 50,184,760 \times 108$	0.79
Sum entropy	$-185,232.39 \pm 270,589.68$	$-298,713.67 \pm 370,598.43$	0.18
Entropy	$-182,814.02 \pm 267,437.51$	$-296,367.58 \pm 368,432.67$	0.18
Difference variance	$33,846 \times 108 \pm 130,551 \times 108$	$33,589 \times 108 \pm 167,868 \times 108$	0.99
Difference entropy	$-191,449.61 \pm 278,782.59$	$-308,046.95 \pm 381,212.79$	0.18
Information correlation	-1.06 ± 0.05	-1.05 ± 0.05	0.63
Autocorrelation	$48,720.01 \pm 80,779.57$	$58,223.44 \pm 55,927.83$	0.65
Dissimilarity	3168.97 ± 5574.98	3216.98 ± 4539.98	0.97
Cluster shade	$-304,126 \times 1015 \pm 1,282,613 \times 1015$	$-388,747 \times 1015 \pm 2,128,824 \times 1015$	0.85
Cluster prominence	$111,513 \times 1021 \pm 481,539 \times 1021$	$1,564,950 \times 1021 \pm 9,594,397 \times 1021$	0.81
Maximum probability	$13,726.16 \pm 19,601.08$	$22,628.46 \pm 26,589.41$	0.15
Inverse difference	1545.88 ± 2747.41	1590.57 ± 2258.06	0.95
RLM-Second level TA parameters			
Short run emphasis	499.27 ± 513.54	781.15 ± 760.76	0.09
Long run emphasis	$105,499.43 \pm 187,431.42$	$173,591.83 \pm 261,588.23$	0.25
Low gray-level emphasis	499.13 ± 513.59	780.58 ± 760.93	0.1
High gray-level emphasis	$105,500 \pm 187,431$	$173,595 \pm 261,586$	0.25
Gray-level nonuniformity	$960,066 \pm 1,724,802$	$2,169,084 \pm 3,480,016$	0.07
Run-length nonuniformity	$6,309,799 \pm 12,683,794$	$13,433,967 \pm 24,658,119$	0.14
Run percentage	0.22 ± 0.14	0.19 ± 0.12	0.5
Short run low gray-level emphasis	404.98 ± 413.67	636.02 ± 636.84	0.09
Long run high gray-level emphasis	$132,195,224 \pm 304,780,688$	$258,271,279 \pm 523,750,848$	0.24
Short run high gray-level emphasis	1584.66 ± 1762.32	2418.38 ± 2386.99	0.13
Long run low gray-level emphasis	1583.89 ± 1762.64	2415.29 ± 2388.21	0.13

Complete responders, TRG1; Non-responders, TRG2–5; GLCM, gray-level color matrix; RLM, run-length matrix

from non-responders, with an area under the ROC curve of 0.86. One study, led by Shu et al. [24], identified multiple T2-weighted texture parameters as potential imaging biomarkers of response to therapy. The authors considered pre-, interim and post-nCRT T2-weighted TA, and found that skewness, entropy and energy of the pre-nCRT TA and variance, kurtosis, energy and entropy of early-nCRT TA (at 3 weeks from the beginning of nCRT) differed significantly between responders and non-responders [24]. Jalil et al. [22] also studied the application of T2-weighted TA in pre- and post-nCRT MRI scans, concluding that this technique can predict patients oncologic outcomes.

Nardone et al. [30] found in 49 patients a correlation between pre-nCRT MRI textural features and early disease progression. Yang et al. [31] found in 76 cases that first-order features of TA extracted from post-nCRT T2-weighted MR images could identify patients with complete response at histopathology. In 2019 and 2020, different authors proposed novel machine learning approaches based on MRI TA, obtaining promising results in the detection of complete

Table 3 Comparison of post-nCRT T2-weighted TA parameters using Student's *t* test

Post-nCRT parameters	Complete responders (mean)	Non-responders (mean)	*p* value
Histograms-First level TA parameters			
Mean	198.85 ± 83.89	170.80 ± 105.31	0.27
Variance	7839.82 ± 5174.08	5314.09 ± 5251.56	0.09
Skewness	1.12 ± 0.50	0.92 ± 0.45	0.13
Excess kurtosis	2.53 ± 2.44	1.79 ± 1.92	0.25
Energy	0.02 ± 0.04	0.01 ± 0.03	0.55
Entropy	3.61 ± 0.56	3.62 ± 0.43	0.92
GLCM-Second level TA parameters			
Energy angular second moment uniformity	$30{,}065{,}178 \pm 68{,}768{,}304$	$123{,}394{,}891 \pm 346{,}998{,}900$	0.10
Contrast inertia variance	570.64 ± 1440.93	726.67 ± 1212.71	0.68
Sum of squares variance	$256{,}618{,}575 \pm 836{,}201{,}520$	$1{,}505{,}819{,}761 \pm 6{,}967{,}958{,}912$	0.25
Homogeneity inverse different moment	3620.78 ± 5811.88	$7368.19 \pm 10{,}036.23$	0.07
Sum average	$10{,}579 \pm 20{,}612$	$18{,}306 \pm 23{,}392$	0.20
Sum variance	$117{,}066 \times 108 \pm 457{,}339 \times 108$	$320{,}607 \times 108 \pm 1{,}537{,}056 \times 108$	0.43
Sum entropy	$-33{,}038 \pm 58{,}400$	$-70{,}390 \pm 107{,}376$	0.08
Entropy	$-32{,}608 \pm 57{,}538$	$-69{,}858 \pm 106{,}792$	0.08
Difference variance	$543 \times 108 \pm 2291 \times 108$	$721 \times 108 \pm 3963 \times 108$	0.82
Difference entropy	$-34{,}334 \pm 61{,}568$	$-71{,}978 \pm 109{,}678$	0.09
Information correlation	-1.06 ± 0.06	-1.04 ± 0.05	0.25
Autocorrelation	$8058.75 \pm 19{,}199.72$	$12{,}190.54 \pm 15{,}813.04$	0.42
Dissimilarity	570.64 ± 1440.93	726.67 ± 1212.71	0.68
Cluster shade	$-980{,}914 \times 1012 \pm 4{,}122{,}723 \times 1012$	$-3{,}486{,}841 \times 1012 \pm 19{,}851{,}861 \times 1012$	0.43
Cluster prominence	$85{,}177 \times 1018 \pm 366{,}845 \times 1018$	$4{,}462{,}584 \times 1018 \pm 2{,}744{,}383 \times 1018$	0.40
Maximum probability	2908.70 ± 4479.32	6514.48 ± 8990.21	**0.04**
Inverse difference	279.43 ± 706.91	358.12 ± 601.43	0.68
RLM-Second level TA parameters			
Short run emphasis	195.95 ± 254.96	314.84 ± 343.11	0.14
Long run emphasis	$13{,}497 \pm 27{,}654$	$30{,}061 \pm 51{,}668$	0.11
Low gray-level emphasis	195.95 ± 254.96	314.40 ± 343.11	0.14
High gray-level emphasis	$13{,}497 \pm 27{,}654$	$30{,}063 \pm 51{,}667$	0.11
Gray-level nonuniformity	$170{,}203 \pm 402{,}923$	$356{,}790 \pm 873{,}277$	0.25
Run-length nonuniformity	$754{,}836 \pm 1{,}993{,}158$	$1{,}804{,}406 \pm 5{,}053{,}533$	0.25
Run percentage	0.23 ± 0.09	0.20 ± 0.07	0.26
Short run low gray-level emphasis	165.33 ± 212.76	264.87 ± 286.67	0.14
Long run high gray-level emphasis	$6{,}708{,}492 \pm 16{,}186{,}486$	$21{,}240{,}783 \pm 52{,}516{,}925$	0.11
Short run high gray-level emphasis	463.31 ± 692.00	809.84 ± 979.01	0.12
Long run low gray-level emphasis	463.31 ± 692.00	807.49 ± 979.29	0.12

Complete responders, TRG1; Non-responders, TRG 2–5; GLCM, gray-level color matrix; RLM, run-length matrix

responders to nCRT [32–37]. Some authors found correlations between MRI TA parameters and mutations status in rectal cancer [38–40] and nodal invasion [41].

The current study tested the efficacy in predicting response to nCRT with TA in 62 patients treated at the same third-level center and restaged with the same MRI scanner with the same protocol, thus conferring a good consistency to our findings. Our results do not support the routinary use of T2-weighted images TA for the evaluation of rectal cancer response to chemoradiation, even if one parameter obtained from MRI images after nCRT showed to be a potential imaging bio-marker to identify patients with a pCR. In fact, among the multiple parameters obtained in both pre- and post-nCRT images, only one, i.e., GLCM maximum probability post-nCRT, showed significant differences between complete responders (i.e., group $0 =$ TRG1) and non-responders (i.e., group $1 =$ TRG2–5). This parameter showed a low sensitivity, although a specificity of 100% was found at the ROC curve Youden index.
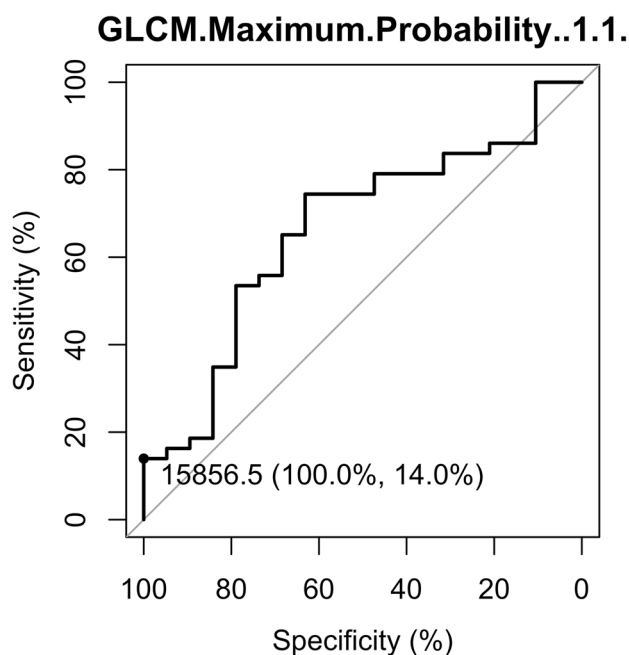
GLCM.Maximum.Probability..1.1.

Fig. 2 GLCM maximum probability ROC curve with Youden index

However, T2-weighted images TA obtained a worse accuracy compared to mrTRG. In the literature, mrTRG1-2 (i.e., complete or very good radiological regression) showed a sensitivity and specificity for predicting cCR of 74.4% and 62.8% respectively [29], and a good correlation to long-term oncologic outcomes [16]. Finally, in our experience, TA proved to be time-spending for the operator, who must use a special software to accurately delineate the tumor circumference in all the MRI slices.

There are several limitations that need to be considered when interpreting our data. The number of patients included in our study is undoubtedly not large enough to draw definitive conclusions, even though many previous studies on MRI TA of rectal cancer have investigated a lower or similar number of cases [20–23, 30, 31]. Also, the retrospective design of the study and the different technique used for MRI examinations (endorectal gel vs. air rectal distension) should be taken into account as potential confounding factors.

In conclusion, we did not find any strong evidence for the use TA as a reliable tool for differentiating TRG1 patients from patients with residual disease. Based on our findings and taking into consideration the complexity of the analysis, we consider MRI T2w texture parameters neither suitable to cover the role of predictors of the histopathological response of rectal cancer patients to neoadjuvant therapy, nor to substitute mrTRG evaluation.

Compliance with ethical standards

References

1. Siegel RL, Miller KD, Fedewa SA, Ahnen DJ, Meester RGS, Barzi A, Jemal A (2017) Colorectal cancer statistics. CA Cancer J Clin 67(3):177–193. https://doi.org/10.3322/caac.21395

2. Benson AB, Venook AP, Al-Hawary MM, Cederquist L, Chen YJ, Ciombor KK, Cohen S, Cooper HS, Deming D, Engstrom PF, Grem JL, Grothey A, Hochster HS, Hoffe S, Hunt S, Kamel A, Kirilcuk N, Krishnamurthi S, Messersmith WA, Meyerhardt J, Mulcahy MF, Murphy JD, Nurkin S, Saltz L, Sharma S, Shibata D, Skibber JM, Sofocleous CT, Stoffel EM, Stotsky-Himelfarb E, Willett CG, Wuthrick E, Gregory KM, Gurski L, Freedman-Cass DA (2018) Rectal cancer, version 2.2018, NCCN clinical practice guidelines in oncology. J Natl Compr Cancer Netw 16(7):874–901. https://doi.org/10.6004/jnccn.2018.0061

3. Dattani M, Heald RJ, Goussous G, Broadhurst J, Sao Juliao GP, Habr-Gama A, Perez RO, Moran BJ (2018) Oncological and survival outcomes in watch and wait patients with a clinical complete response after neoadjuvant chemoradiotherapy for rectal cancer: a systematic review and pooled analysis. Ann Surg 268(6):955–967. https://doi.org/10.1097/sla.0000000000002761

4. Maas M, Beets-Tan RG, Lambregts DM, Lammering G, Nelemans PJ, Engelen SM, van Dam RM, Jansen RL, Sosef M, Leijtens JW, Hulsewe KW, Buijsen J, Beets GL (2011) Wait-and-see policy for clinical complete responders after chemoradiation for rectal cancer. J Clin Oncol 29(35):4633–4640. https://doi.org/10.1200/jco.2011.37.7176

5. Pucciarelli S, Del Bianco P, Efficace F, Serpentini S, Capirci C, De Paoli A, Amato A, Cuicchi D, Nitti D (2011) Patient-reported outcomes after neoadjuvant chemoradiotherapy for rectal cancer: a multicenter prospective observational study. Ann Surg 253(1):71–77. https://doi.org/10.1097/SLA.0b013e3181fcb856

6. Campayo M, Navarro A, Benítez JC, Santasusagna S, Ferrer C, Monzó M, Cirera L (2018) miR-21, miR-99b and miR-375 combination as predictive response signature for preoperative chemoradiotherapy in rectal cancer. PLoS ONE 13(11):e0206542. https://doi.org/10.1371/journal.pone.0206542

7. Rampazzo E, Del Bianco P, Bertorelle R, Boso C, Perin A, Spiro G, Bergamo F, Belluco C, Buonadonna A, Palazzari E, Lonardi S,

De Paoli A, Pucciarelli S, De Rossi A (2018) The predictive and prognostic potential of plasma telomerase reverse transcriptase (TERT) RNA in rectal cancer patients. Br J Cancer 118(6):878–886. https://doi.org/10.1038/bjc.2017.492

8. van der Sande ME, Maas M, Melenhorst J, Breukink SO, van Leerdam ME, Beets GL (2019) Predictive value of endoscopic features for a complete response after chemoradiotherapy for rectal cancer. Ann Surg. https://doi.org/10.1097/sla.0000000000003718

9. Ko HM, Choi YH, Lee JE, Lee KH, Kim JY, Kim JS (2019) Combination assessment of clinical complete response of patients with rectal cancer following chemoradiotherapy with endoscopy and magnetic resonance imaging. Ann Coloproctol 35(4):202–208. https://doi.org/10.3393/ac.2018.10.15

10. Lambregts DMJ, Boellaard TN, Beets-Tan RGH (2019) Response evaluation after neoadjuvant treatment for rectal cancer using modern MR imaging: a pictorial review. Insights Imaging 10(1):15. https://doi.org/10.1186/s13244-019-0706-x

11. Battersby NJ, Balyasnikova S, Brown G (2014) Guiding post-treatment decisions in rectal cancer: mrTRG is a practical place to start. Oncology (Williston Park) 28(8):677–680

12. Mandard A-M, Dalibard F, Mandard J-C, Marnay J, Henry-Amar M, Petiot J-F, Roussel A, Jacob J-H, Segol P, Samama G, Ollivier J-M, Bonvalot S, Gignoux M (1994) Pathologic assessment of tumor regression after preoperative chemoradiotherapy of esophageal carcinoma. Clinicopathologic correlations. Cancer 73(11):2680–2686. https://doi.org/10.1002/1097-0142(19940601)73:11<2680:Aid-cncr2820731105>3.0.Co;2-c

13. Patel UB, Brown G, Rutten H, West N, Sebag-Montefiore D, Glynne-Jones R, Rullier E, Peeters M, Van Cutsem E, Ricci S, Van de Velde C, Kjell P, Quirke P (2012) Comparison of magnetic resonance imaging and histopathological response to chemoradiotherapy in locally advanced rectal cancer. Ann Surg Oncol 19(9):2842–2852. https://doi.org/10.1245/s10434-012-2309-3

14. Trakarnsanga A, Gönen M, Shia J, Nash GM, Temple LK, Guillem JG, Paty PB, Goodman KA, Wu A, Gollub M, Segal N, Saltz L, Garcia-Aguilar J, Weiser MR (2014) Comparison of tumor regression grade systems for locally advanced rectal cancer after multimodality treatment. J Natl Cancer Inst. https://doi.org/10.1093/jnci/dju248

15. Siddiqui MR, Bhoday J, Battersby NJ, Chand M, West NP, Abulafi AM, Tekkis PP, Brown G (2016) Defining response to radiotherapy in rectal cancer using magnetic resonance imaging and histopathological scales. World J Gastroenterol 22(37):8414–8434. https://doi.org/10.3748/wjg.v22.i37.8414

16. Sclafani F, Brown G, Cunningham D, Wotherspoon A, Tait D, Peckitt C, Evans J, Yu S, Sena Teixeira Mendes L, Tabernero J, Glimelius B, Cervantes A, Thomas J, Begum R, Oates J, Chau I (2016) PAN-EX: a pooled analysis of two trials of neoadjuvant chemotherapy followed by chemoradiotherapy in MRI-defined, locally advanced rectal cancer. Ann Oncol 27(8):1557–1565. https://doi.org/10.1093/annonc/mdw215

17. Siddiqui MR, Gormly KL, Bhoday J, Balyansikova S, Battersby NJ, Chand M, Rao S, Tekkis P, Abulafi AM, Brown G (2016) Interobserver agreement of radiologists assessing the response of rectal cancers to preoperative chemoradiation using the MRI tumour regression grading (mrTRG). Clin Radiol 71(9):854–862. https://doi.org/10.1016/j.crad.2016.05.005

18. Rengo M, Picchia S, Marzi S, Bellini D, Caruso D, Caterino M, Ciolina M, De Santis D, Musio D, Tombolini V, Laghi A (2017) Magnetic resonance tumor regression grade (MR-TRG) to assess pathological complete response following neoadjuvant radiochemotherapy in locally advanced rectal cancer. Oncotarget 8(70):114746–114755. https://doi.org/10.18632/oncotarget.21778

19. Taylor FG, Quirke P, Heald RJ, Moran B, Blomqvist L, Swift I, Sebag-Montefiore DJ, Tekkis P, Brown G (2011) Preoperative high-resolution magnetic resonance imaging can identify good prognosis stage I, II, and III rectal cancer best managed by surgery alone: a prospective, multicenter, European study. Ann Surg 253(4):711–719. https://doi.org/10.1097/SLA.0b013e31820b8d52

20. De Cecco CN, Ganeshan B, Ciolina M, Rengo M, Meinel FG, Musio D, De Felice F, Raffetto N, Tombolini V, Laghi A (2015) Texture analysis as imaging biomarker of tumoral response to neoadjuvant chemoradiotherapy in rectal cancer patients studied with 3-T magnetic resonance. Invest Radiol 50(4):239–245. https://doi.org/10.1097/rli.0000000000000116

21. De Cecco CN, Ciolina M, Caruso D, Rengo M, Ganeshan B, Meinel FG, Musio D, De Felice F, Tombolini V, Laghi A (2016) Performance of diffusion-weighted imaging, perfusion imaging, and texture analysis in predicting tumoral response to neoadjuvant chemoradiotherapy in rectal cancer patients studied with 3T MR: initial experience. Abdom Radiol (NY) 41(9):1728–1735. https://doi.org/10.1007/s00261-016-0733-8

22. Jalil O, Afaq A, Ganeshan B, Patel UB, Boone D, Endozo R, Groves A, Sizer B, Arulampalam T (2017) Magnetic resonance based texture parameters as potential imaging biomarkers for predicting long-term survival in locally advanced rectal cancer treated by chemoradiotherapy. Colorectal Dis 19(4):349–362. https://doi.org/10.1111/codi.13496

23. Giannini V, Mazzetti S, Bertotto I, Chiarenza C, Cauda S, Delmastro E, Bracco C, Di Dia A, Leone F, Medico E, Pisacane A, Ribero D, Stasi M, Regge D (2019) Predicting locally advanced rectal cancer response to neoadjuvant therapy with ^{18}F-FDG PET and MRI radiomics features. Eur J Nucl Med Mol Imaging 46(4):878–888. https://doi.org/10.1007/s00259-018-4250-6

24. Shu Z, Fang S, Ye Q, Mao D, Cao H, Pang P, Gong X (2019) Prediction of efficacy of neoadjuvant chemoradiotherapy for rectal cancer: the value of texture analysis of magnetic resonance images. Abdom Radiol (NY) 44(11):3775–3784. https://doi.org/10.1007/s00261-019-01971-y

25. Lu Z, Wang L, Xia K, Jiang H, Weng X, Jiang J, Wu M (2019) Prediction of clinical pathologic prognostic factors for rectal adenocarcinoma: volumetric texture analysis based on apparent diffusion coefficient maps. J Med Syst 43(12):331. https://doi.org/10.1007/s10916-019-1464-5

26. R Development Core Team (2017) R: a language and environment for statistical computing. R Foundation for Statistical Computing, Vienna

27. Meyer-Baese A, Schmid V (2014) Pattern recognition and signal analysis in medical imaging. Elsevier, Amsterdam

28. Demler OV, Pencina MJ, D'Agostino RB Sr (2012) Misuse of DeLong test to compare AUCs for nested models. Stat Med 31(23):2577–2587. https://doi.org/10.1002/sim.5328

29. Sclafani F, Brown G, Cunningham D, Wotherspoon A, Mendes LST, Balyasnikova S, Evans J, Peckitt C, Begum R, Tait D, Tabernero J, Glimelius B, Roselló S, Thomas J, Oates J, Chau I (2017) Comparison between MRI and pathology in the assessment of tumour regression grade in rectal cancer. Br J Cancer 117(10):1478–1485. https://doi.org/10.1038/bjc.2017.320

30. Nardone V, Reginelli A, Scala F, Carbone SF, Mazzei MA, Sebaste L, Carfagno T, Battaglia G, Pastina P, Correale P, Tini P, Pellino G, Cappabianca S, Pirtoli L (2019) Magnetic-resonance-imaging texture analysis predicts early progression in rectal cancer patients undergoing neoadjuvant chemoradiation. Gastroenterol Res Pract 2019:8505798. https://doi.org/10.1155/2019/8505798

31. Yang L, Qiu M, Xia C, Li Z, Wang Z, Zhou X, Wu B (2019) Value of high-resolution DWI in combination with texture analysis for the evaluation of tumor response after preoperative chemoradiotherapy for locally advanced rectal cancer. AJR Am J Roentgenol 212:1–8. https://doi.org/10.2214/ajr.18.20689

32. Shi L, Zhang Y, Nie K, Sun X, Niu T, Yue N, Kwong T, Chang P, Chow D, Chen JH, Su MY (2019) Machine learning for prediction of chemoradiation therapy response in rectal cancer using pre-treatment and mid-radiation multi-parametric MRI. Magn Reson Imaging 61:33–40. https://doi.org/10.1016/j.mri.2019.05.003

33. Shayesteh SP, Alikhassi A, Fard Esfahani A, Miraie M, Geramifar P, Bitarafan-Rajabi A, Haddad P (2019) Neo-adjuvant chemoradiotherapy response prediction using MRI based ensemble learning method in rectal cancer patients. Phys Med 62:111–119. https://doi.org/10.1016/j.ejmp.2019.03.013

34. Ferrari R, Mancini-Terracciano C, Voena C, Rengo M, Zerunian M, Ciardiello A, Grasso S, Mare V, Paramatti R, Russomando A, Santacesaria R, Satta A, Solfaroli Camillocci E, Faccini R, Laghi A (2019) MR-based artificial intelligence model to assess response to therapy in locally advanced rectal cancer. Eur J Radiol 118:1–9. https://doi.org/10.1016/j.ejrad.2019.06.013

35. Shayesteh SP, Alikhassi A, Farhan F, Gahletaki R, Soltanabadi M, Haddad P, Bitarafan-Rajabi A (2019) Prediction of response to neoadjuvant chemoradiotherapy by MRI-based machine learning texture analysis in rectal cancer patients. J Gastrointest Cancer. https://doi.org/10.1007/s12029-019-00291-0

36. van Griethuysen JJM, Lambregts DMJ, Trebeschi S, Lahaye MJ, Bakers FCH, Vliegen RFA, Beets GL, Aerts H, Beets-Tan RGH (2020) Radiomics performs comparable to morphologic assessment by expert radiologists for prediction of response to neoadjuvant chemoradiotherapy on baseline staging MRI in rectal cancer. Abdom Radiol (NY) 45(3):632–643. https://doi.org/10.1007/s00261-019-02321-8

37. Antunes JT, Ofshteyn A, Bera K, Wang EY, Brady JT, Willis JE, Friedman KA, Marderstein EL, Kalady MF, Stein SL, Purysko AS, Paspulati R, Gollamudi J, Madabhushi A, Viswanath SE (2020) Radiomic features of primary rectal cancers on baseline T2-weighted MRI are associated with pathologic complete response to neoadjuvant chemoradiation: a multisite study. J Magn Reson Imaging. https://doi.org/10.1002/jmri.27140

38. Horvat N, Veeraraghavan H, Pelossof RA, Fernandes MC, Arora A, Khan M, Marco M, Cheng CT, Gonen M, Golia Pernicka JS, Gollub MJ, Garcia-Aguillar J, Petkovska I (2019) Radiogenomics of rectal adenocarcinoma in the era of precision medicine: a pilot study of associations between qualitative and quantitative MRI imaging features and genetic mutations. Eur J Radiol 113:174–181. https://doi.org/10.1016/j.ejrad.2019.02.022

39. Oh JE, Kim MJ, Lee J, Hur BY, Kim B, Kim DY, Baek JY, Chang HJ, Park SC, Oh JH, Cho SA, Sohn DK (2020) Magnetic resonance-based texture analysis differentiating KRAS mutation status in rectal cancer. Cancer Res Treat 52(1):51–59. https://doi.org/10.4143/crt.2019.050

40. Xu Y, Xu Q, Ma Y, Duan J, Zhang H, Liu T, Li L, Sun H, Shi K, Xie S, Wang W (2019) Characterizing MRI features of rectal cancers with different KRAS status. BMC Cancer 19(1):1111. https://doi.org/10.1186/s12885-019-6341-6

41. Yang L, Liu D, Fang X, Wang Z, Xing Y, Ma L, Wu B (2019) Rectal cancer: can T2WI histogram of the primary tumor help predict the existence of lymph node metastasis? Eur Radiol 29(12):6469–6476. https://doi.org/10.1007/s00330-019-06328-z